

# Hyaluronan preconditioning of monocytes/macrophages affects their angiogenic behavior and regulation of TSG-6 expression in a tumor type-specific manner

Fiorella M. Spinelli<sup>1</sup>, Daiana L. Vitale<sup>1</sup>, Antonella Icardi<sup>1</sup>, Ilaria Caon<sup>2</sup>, Alejandra Brandone<sup>3</sup>, Paula Giannoni<sup>4</sup>, Virginia Saturno<sup>3</sup>, Alberto Passi<sup>2</sup>, Mariana García<sup>5</sup>, Ina Sevic<sup>1</sup> and Laura Alaniz<sup>1</sup>

1 Laboratorio de Microambiente Tumoral, Centro de Investigaciones Básicas y Aplicadas (CIBA), Universidad Nacional de la Pcia. de Bs. As. Centro de Investigaciones y Transferencia del Noroeste de la Pcia. de Bs. As. (CIT NOBA, UNNOBA-CONICET), Junín, Argentina

2 Dipartimento di Medicina e Chirurgia, Università degli Studi dell'Insubria, Varese, Italia

3 Hospital Interzonal General de Agudos Dr. Abraham F. Piñeyro, Junín, Argentina

4 Clínica Centro, Junín, Argentina

5 Laboratorio de Terapia Génica, IIMT – CONICET, Universidad Austral, Derqui-Pilar, Argentina

## Keywords

angiogenesis; breast carcinoma; colorectal carcinoma; hyaluronan; monocytes/macrophages; TSG-6

## Correspondence

L. Alaniz, Laboratorio de Microambiente Tumoral, Centro de Investigaciones Básicas y Aplicadas (CIBA), UNNOBA, CIT NOBA (UNNOBA-CONICET), Jorge Newbery 261, Junín, Buenos Aires B6000, Argentina  
 Tel: +54 236 4 407750 ext 11620  
 E-mail: lalaniz@comunidad.unnoba.edu.ar

(Received 12 August 2018, revised 18 March 2019, accepted 29 April 2019)

doi:10.1111/febs.14871

Hyaluronan is a glycosaminoglycan normally present in the extracellular matrix in most tissues. Hyaluronan is a crucial player in many processes associated with cancer, such as angiogenesis, invasion, and metastasis. However, little has been reported regarding the action of hyaluronan on monocytes/macrophages (Mo/MØ) in tumor angiogenesis and its consequences on tumor development. In the present study, we investigated the effects of hyaluronan of different sizes on human Mo/MØ angiogenic behavior in colorectal and breast carcinoma. *In vitro*, the treatment of Mo/MØ with lysates and conditioned media from a breast but not from colorectal carcinoma cell line plus high-molecular weight hyaluronan induced: (a) an increased expression of angiogenic factors VEGF, IL-8, FGF-2, and MMP-2, (b) an increased endothelial cell migration, and (c) a differential expression of hyaluronan-binding protein TSG-6. Similar results were observed in Mo/MØ derived from breast cancer patients treated with tumor lysates. Besides, macrophages primed with high-molecular weight hyaluronan and inoculated in human breast cancer xenograft tumor increased blood vessel formation and diminished TSG-6 levels. In contrast, the effects triggered by high-molecular weight hyaluronan on Mo/MØ in breast cancer context were not observed in the context of colorectal carcinoma. Taken together, these results indicate that the effect of high-molecular weight hyaluronan as an inductor of the angiogenic behavior of macrophages in breast tumor context is in part consequence of the presence of TSG-6.

## Introduction

Hyaluronan (HA), an anionic non-sulfated glycosaminoglycan, is a main component of the extracellular matrix in tissues. HA functions are well known to be size dependent. At homeostasis, high-

## Abbreviations

BC, basal control; CM, conditioned media; ECs, endothelial cells; HA, hyaluronan; HMW, high-molecular weight; LCM, LoVo-conditioned media; LMW, low-molecular weight; LTL, LoVo tumor cell lysate; MCM, MDA-MB-231-conditioned media; MØ, macrophages; Mo, monocytes; MTL, MDA-MB 231 tumor cell lysate; NATL, normal tissue adjacent to the tumor lysate; NRQ, normalized relative quantities; PBMCs, peripheral blood mononuclear cells; TL, tumor cell lysate; TSG-6, tumor necrosis factor (TNF)-stimulated gene 6; TTL, tumor tissue lysate.

molecular weight HA (HMW HA: 1500–1800 kDa) is predominant and has hydrodynamic properties, whereas low-molecular weight HA (LMW HA: 100–300 kDa) is present mainly during inflammation [1]. It is well known that HA binds several cell surface receptors such as CD44, TLR4, and RHAMM and its size can influence the receptor activation and downstream signaling [2]. Even more, tumor necrosis factor (TNF)-stimulated gene 6 (TSG-6) is a HA-binding protein. TSG-6 has a crucial role in the formation of HA cross-linking with other matrix components, such as the serine protease inhibitor inter- $\alpha$ -inhibitor (I $\alpha$ I) heavy chains (HCs), which allow the stabilization and structural integrity of the extracellular matrix [3–5].

Hyaluronan is a crucial player in many processes associated with cancer [6] and has been detected in tissues [6] as well as serum, in multiple types of cancer [7]. Particularly, HA was detected in serum from breast cancer patients [8,9]. In several tumors, LMW HA promotes spreading by stimulating angiogenesis and creating a microvascular network [10]. However, we have previously demonstrated that, in colorectal carcinoma, exogenous LMW but not HMW HA significantly reduced tumor growth *in vitro* and *in vivo*, in part by its immunostimulatory action [11]. Although in breast carcinoma, LMW HA and not HMW HA may contribute to tumor progression [12]. These controversial results might be due to not considering the impact on tumor-associated cells such as monocytes/macrophages (Mo/MØ) and factors that modulate HA structure and function.

Monocytes (Mo) are circulating innate immune cells. Some monocytes migrate into tissues or to the sites of damage or infection where they subsequently develop into different type of monocyte-derived macrophages (MØ). Cells of this lineage are jointly described to as mononuclear phagocytes or Mo/MØ [13]. These cells participate in many states of physiological and pathological processes, in addition to their role in the immune response [14]. MØ are critical modulators of the tumor microenvironment, although its behavior differs considerably among tumors. They are classically known as tumor-associated macrophage (TAM) and considered an M2 type or regulatory MØ, which are able to promote angiogenesis [15]. Mo/MØ are able to bind HA which induces intracellular signals [16,17]; however, the role that different-sized HA plays on MØ behavior in the presence of tumor factors is not well known, defining their anti- or pro-tumor effect. Moreover, TSG-6 is not, in general, a constitutively expressed protein in normal adult tissues, and during inflammation, its expression is upregulated. This HA-binding protein is produced by an activated MØ-modulating inflammation process as a

consequence of tissue injury [5,18,19]. However, its mechanism of action and its role in Mo/MØ behavior are not fully understood in cancer. Consequently, the aim of our work was to evaluate HA (LMW and HMW) effect on human Mo/MØ angiogenic behavior in two different tumor microenvironments, colorectal and breast. It is well known that tumor necrosis is related to a more angiogenic and inflammatory microenvironment in various types of cancer [20,21], among them breast cancer [22]. That is why we evaluated Mo/MØ behavior exposed to factors from tumor cell lysates or cell supernatants. We analyzed the role of TSG-6 as a modulator of HA function within these tumor microenvironments.

## Results

### HA fails to modulate phenotypic markers of Mo/MØ in tumor microenvironments

To characterize peripheral blood mononuclear cell (PBMC)-derived Mo/MØ by the expression of cell surface antigens, we evaluated by flow cytometry different cell surface markers: CD14, HLA, CD80, and CD206. Monocytes were gated by CD14-positive expression and the co-expression of the markers was analyzed to immune characterize Mo/MØ. On average, 81% of the cells in culture expressed this marker, indicating a higher homogeneity of the culture and their monocytic lineage (Fig. 1). Besides, no differences were found between treatments. HA (HMW or LMW) and factors from tumor cell lysates (TL) were not able to modulate the expression of these molecules in our experimental conditions (Fig. 1A). Similar results were observed during treatment of macrophages exposed to conditioned media (CM) (Fig. 1B). TL and CM concentration does not affect Mo/MØ viability (Fig. 2). Therefore, HA plus TL or CM were not able to modulate the Mo/MØ surface markers. Since our aim was to study the modulation of HA on Mo/MØ angiogenic function in tumor context, we analyzed the expression of pro-angiogenic molecules: VEGF, FGF-2, IL-8, and MMPs.

### HMW HA increased VEGF production in Mo/MØ in breast but not in colorectal carcinoma microenvironment

As mentioned previously, TAMs induce tumor vascularization by releasing several factors, including VEGF which is the main angiogenic factor. Thus, VEGF expression was analyzed to evaluate the effect of HA (LMW and HMW) on Mo/MØ pulsed with TL from breast cancer cell line MDA-MB-231 (MTL) or colorectal carcinoma cell line LoVo (LTL). Mo/MØ

treated with MTL plus HMW HA significantly increased VEGF levels (NRQ:  $3.769 \pm 0.9416$ ) when compared to MTL without HA (NRQ:  $0.3000 \pm 0.1732$ ) or MTL plus LMW HA (NRQ:  $0.3587 \pm 0.2071$ ) (Fig. 3A). No differences were observed between treatments with LTL (Fig. 3A). In order to evaluate VEGF expression modulated by CM, we performed a RT-qPCR. Mo/MØ were treated with CM derived from MDA-MB-231 (MCM) or LoVo (LCM). VEGF levels increased when Mo/MØ were treated with MCM plus HMW HA (NRQ:  $3.216 \pm 0.06561$ ) in comparison with MCM treatment without HA (NRQ:  $0.1100 \pm 0.0110$ ) and plus LMW HA (NRQ:  $0.0 \pm 0.0$ ) (Fig. 3B). Mo/MØ treated with LCM plus HA (LMW or HMW) showed no differences in VEGF expression levels. Taken together, these results indicate that HMW HA is able to increase VEGF levels in Mo/MØ in a breast carcinoma context.

### HMW HA increased the expression of IL-8 and FGF-2 in Mo/MØ in breast but not in colorectal carcinoma microenvironment

Mo/MØ express and secrete other important angiogenic factors, like IL-8 and FGF-2. Consequently, we evaluated the mRNA expression levels of IL-8 and FGF-2 of Mo/MØ pulsed with TL or CM with or without HA. In concordance with VEGF synthesis levels, Mo/MØ incubated with MTL plus HMW HA

increased IL-8 expression levels (NRQ:  $5.761 \pm 1.461$ ) when compared to the treatments with MTL without HA (NRQ:  $2.630 \pm 0.5698$ ) or MTL plus LMW HA (NRQ:  $1.756 \pm 0.1945$ ) (Fig. 3C). When we analyzed IL-8 levels from Mo/MØ treated with CM, we observed a significant increase in IL-8 with the treatment with MCM plus HMW HA (NRQ:  $10.61 \pm 0.4400$ ) (Fig. 3D). FGF-2 expression levels in Mo/MØ treated with MTL plus HMW HA (NRQ:  $2.972 \pm 0.8020$ ) showed an increased tendency when compared to MTL without HA (NRQ:  $2.461 \pm 0.5345$ ) and a significant increase comparing to basal control (BC; NRQ:  $0.3447 \pm 0.09539$ ) (Fig. 3E). Similarly, Mo/MØ treated with HMW HA plus MCM increased FGF-2 expression levels (NRQ:  $4.150 \pm 0.2656$ ) comparing to MCM (NRQ:  $2.280 \pm 0.3600$ ) and MCM plus LMW HA (NRQ:  $0.9050 \pm 0.3650$ ) (Fig. 3F). Mo/MØ treated with LTL or LCM plus HA (LMW or HMW) showed no differences in the mRNA expression levels of IL-8 and FGF-2 (Fig. 3C–F).

### HMW HA treatment modulated MMPs expression levels and activity in Mo/MØ in a breast but not in colorectal carcinoma microenvironment

In tumor context, Mo/MØ upregulate MMP-2 and MMP-9 production and their proteolytic activity

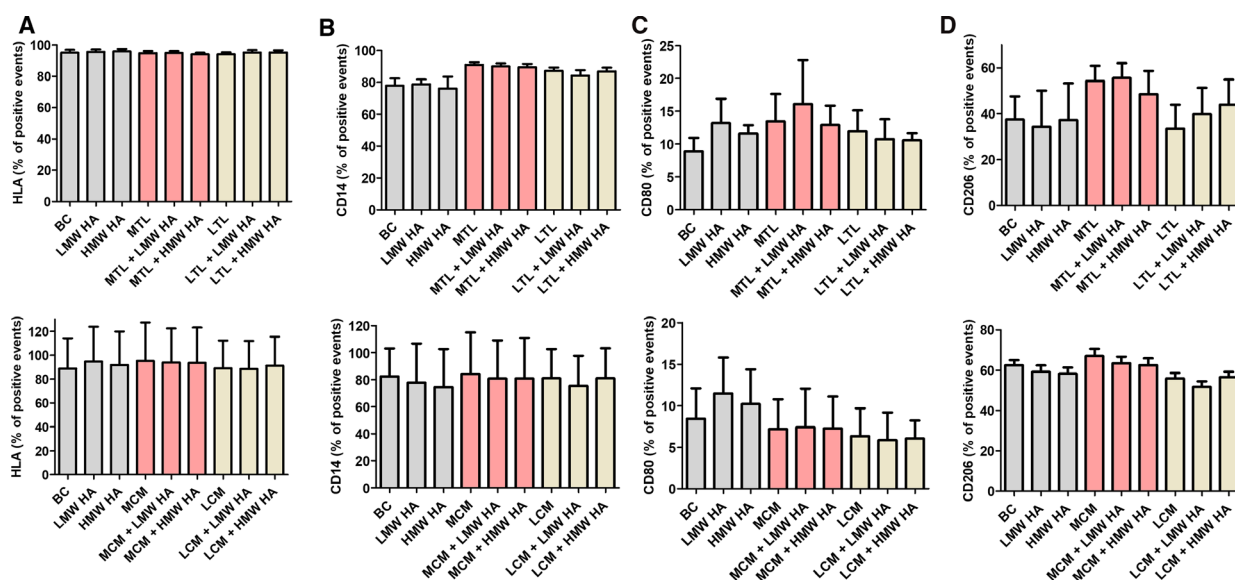


**Fig. 1.** Characterization of Mo/MØ by Flow Cytometry. Mo/MØ culture treatments stained with mAbs anti A) HLA, B) CD14, C) CD80 and D) CD206, upper panel are tumor lysates (TL) treatments and lower panel conditioned media treatments. Mo/MØ were gated and the co-expression of the markers were analyzed. Data are expressed as mean percentage  $\pm$  SEM from three independent experiments. Data was analyzed through one-way ANOVA analysis. BC = basal control; LMW HA = low molecular weight hyaluronan; HMW HA = high molecular weight hyaluronan; MTL = MDA-MB-231 tumor cell lysate; LTL = LoVo tumor cell lysate.

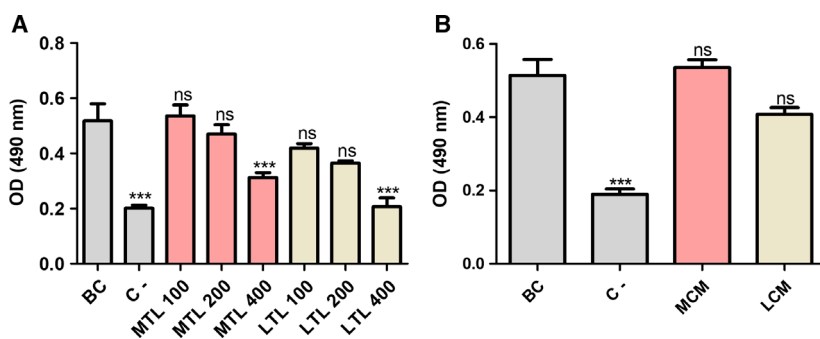


**Fig. 2.** Cell viability. Mo/MØ were cultured with (A) different concentrations of MTL or LTL and (B) MCM or LCM, and cell viability was measured using MTS assay. Data are expressed as OD mean  $\pm$  SEM from three independent experiments. \*\*\* $P$  < 0.001 vs. control, one-way ANOVA analysis. C-, negative control, cell death was induced.

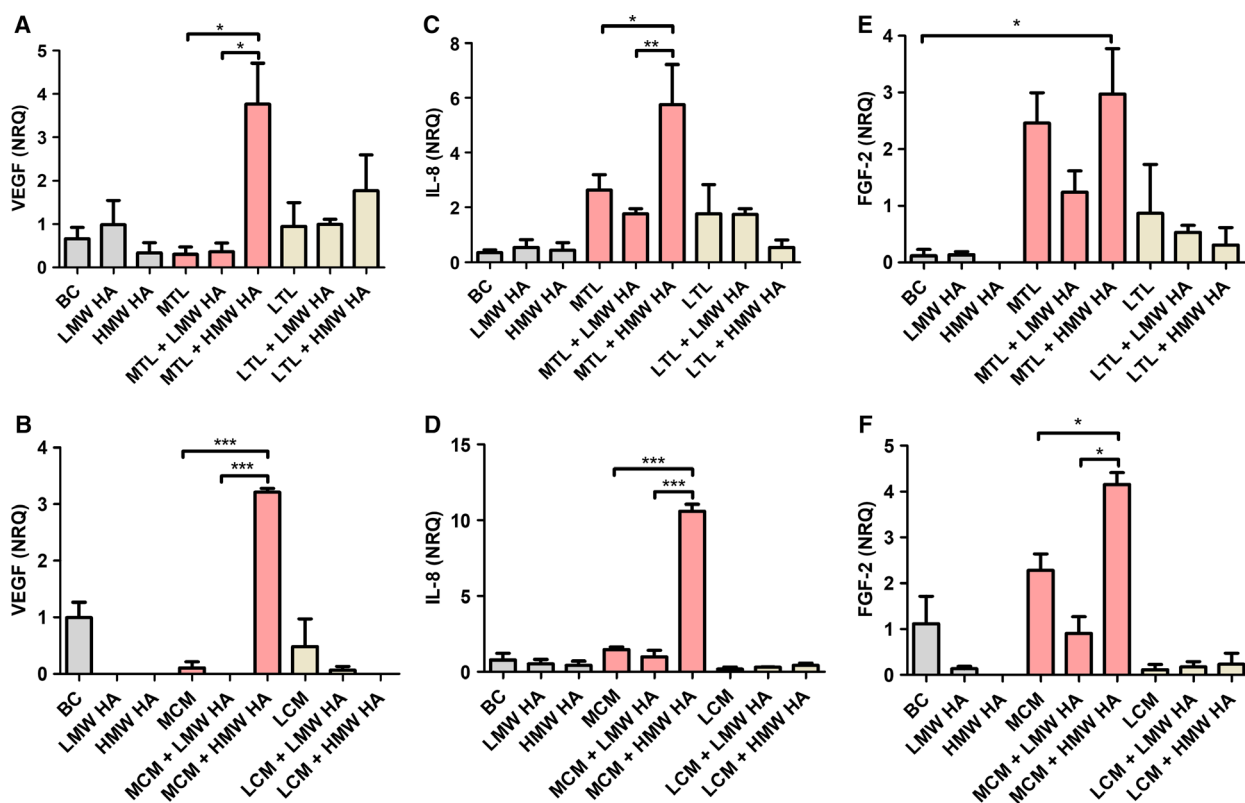


**Fig. 3.** *In vitro* angiogenesis in Mo/MØ treated with HA. (A, B) VEGF, (C, D) IL-8, and (E, F) FGF-2 mRNA expression levels were measured by RT-qPCR in Mo/MØ. Data are expressed as normalized relative quantities (NRQ) mean  $\pm$  SEM, from three independent experiments. \* $P$  < 0.05, \*\* $P$  < 0.01, and \*\*\* $P$  < 0.001, one-way ANOVA analysis.

triggers the degradation of the extracellular matrix and the bioavailability of angiogenic factors [23]. Thus, we analyzed MMPs activity by gelatin zymography as another angiogenic mechanism regulated by HA. MMP-9 activity showed no difference between HA treatments with TL and CM (Fig. 4A,E) in Mo/MØ. However, the treatment with MTL plus HMW HA increased MMP-2 activity (NRQ:  $5.685 \pm 0.2162$ ) in these cells (Fig. 4C) compared to BC. The HA action

was not only restricted to HMW HA, the treatment with MTL plus LMW HA also increased its activity (NRQ:  $6.278 \pm 0.5816$ ) (Fig. 4C). MMP-2 showed similar activity in Mo/MØ PBMCs pulsed with LTL both treatments and controls (Fig. 4C). In addition, to corroborate these results, we analyzed mRNA levels of MMP-9 and MMP-2. As expected, MMP-9 expression levels showed no differences during the treatments (Fig. 4B). MMP-2 mRNA levels significantly increased

with MTL plus HMW HA treatment (NRQ:  $5.685 \pm 0.2162$ ) with respect to MTL (NRQ:  $3.343 \pm 1.220$ ) (Fig. 4D). MCM or LCM treatments of Mo/MØ did not modulate MMPs activity or their expression levels (Fig. 4F,H).

### Higher *in vitro* migration of ECs toward Mo/MØ supernatants when treated with HMW HA in a breast but not in colorectal carcinoma microenvironment

We decided to test the migration of ECs *in vitro*, as a way of evaluating the functional modulation of these cells involved in the vessel formation. As expected, significantly higher migration of ECs was observed toward the supernatants of Mo/MØ treated with MTL plus HMW HA (index cell migration:  $6.830 \pm 1.465$ ) when compared to MTL without HA (index cell migration:  $3.523 \pm 0.5100$ ) and MTL plus LMW HA

(index cell migration:  $1.380 \pm 0.2287$ ) (Fig. 5). However, the treatments of Mo/MØ with LCM showed no differences in the migration levels of ECs (Fig. 5). Moreover, differential migration was observed in ECs toward Mo/MØ supernatants derived in the presence of MTL (index cell migration:  $3.523 \pm 0.5100$ ) when compared with LTL (index cell migration:  $0.7459 \pm 0.1051$ ). We were not able to perform this experiment with tumor cell CM since MCM as well as LCM are chemoattractants of ECs *per se* and did not allow us to evaluate differences among the treatments.

### Mo/MØ treated with HMW HA modulated HA receptors' expression levels in a breast carcinoma microenvironment

Hyaluronan induces cell signaling through several receptors such as CD44, TLR-4, and RHAMM. Since these receptors are involved in HA responses in Mo/

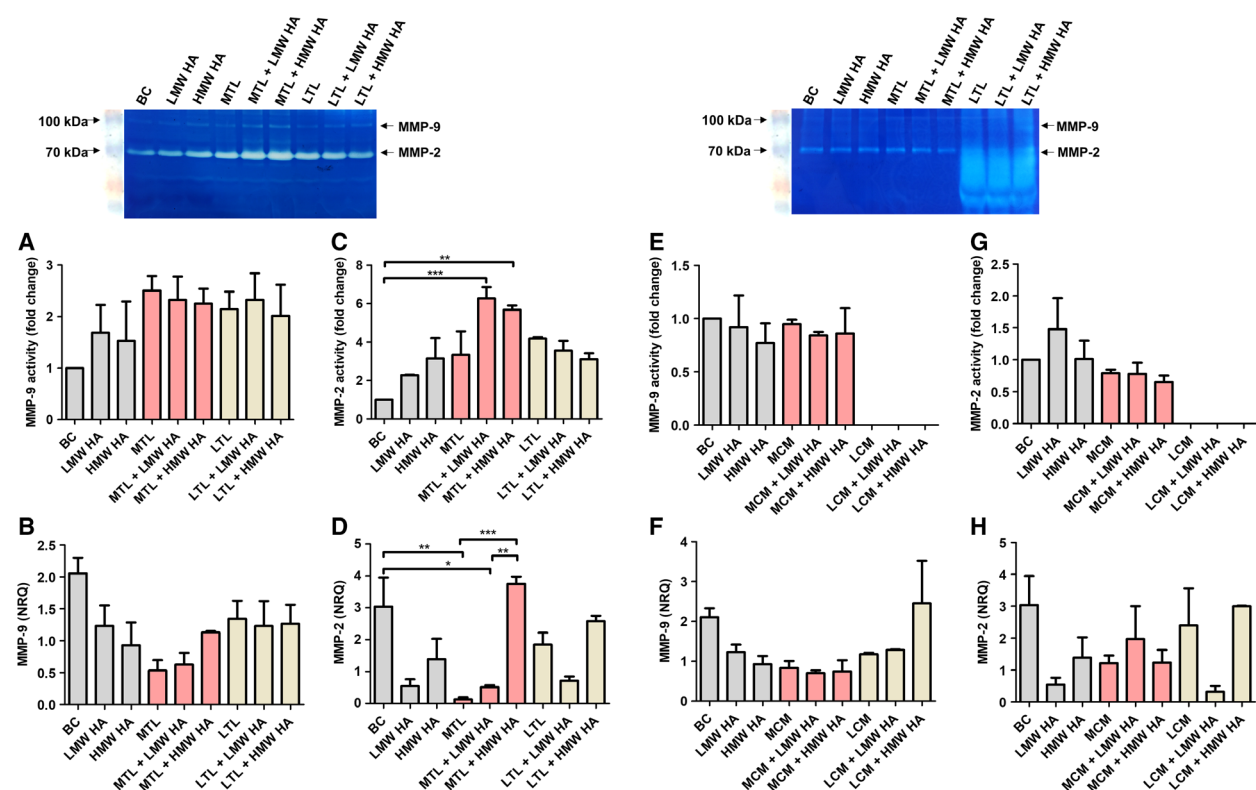


**Fig. 4.** MMPs activity and mRNA levels in Mo/MØ treated with HA. (A, C, E, G). MMPs activity was analyzed by gelatin zymography. MMP-2 activity in Mo/MØ supernatants treated with TL (C) or CM (G) and HA (LWW and HMW). MMP-9 activity in Mo/MØ supernatants treated with TL (A) or CM (E) and HA (LWW and HMW). The activity was quantified by densitometry and relative activity was obtained by normalizing values to untreated samples. Data are expressed as fold change mean  $\pm$  SEM and correspond to three independent experiments. (B, D, F, H) mRNA expression levels measured by RT-qPCR. MMP-2 mRNA levels in Mo/MØ supernatants treated with TL (D) or CM (H) and HA (LWW and HMW) and MMP-9 mRNA levels in Mo/MØ supernatants treated with TL (B) or CM (F) and HA (LWW and HMW) Data are expressed as normalized relative quantities (NRQ) mean  $\pm$  SEM, from three independent experiments. \* $P < 0.05$ , \*\* $P < 0.01$ , and \*\*\* $P < 0.001$ , one-way ANOVA analysis.

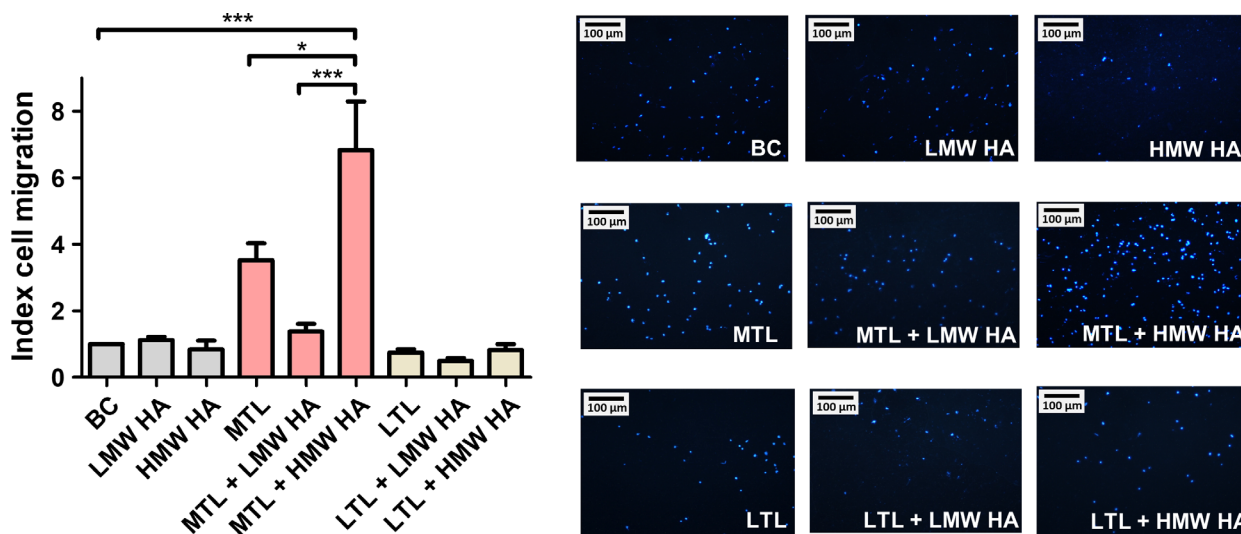


**Fig. 5.** Endothelial cells migration toward Mo/MØ supernatants treated with HA. Results are expressed as an index of cell migration with respect to nontreated BC ± SEM from three representative visual fields. Results are representative of three independent experiments. \* $P < 0.05$  and \*\*\* $P < 0.001$ , one-way ANOVA analysis.

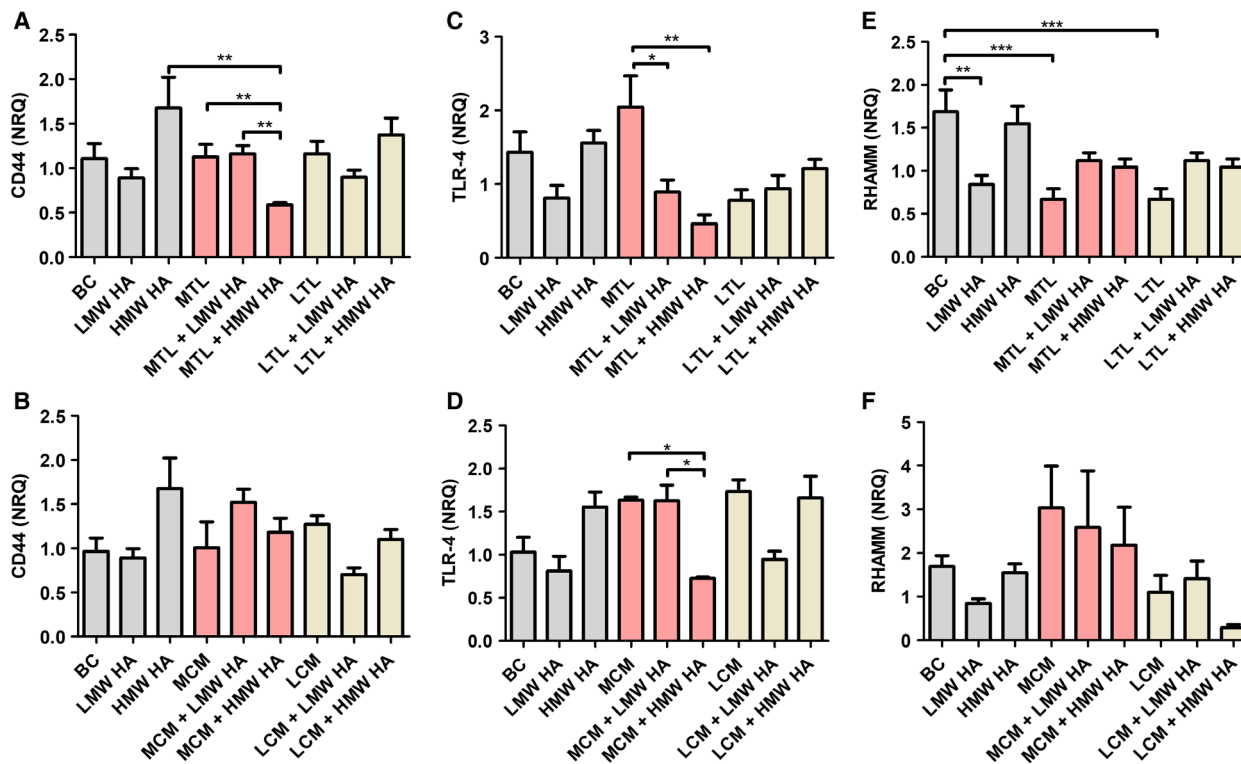


**Fig. 6.** HA receptors mRNA levels in Mo/MØ treated with HA. (A–F) CD44, TLR-4, RHAMM mRNA expression levels measured by RT-qPCR mRNA levels measured by RT-qPCR in Mo/MØ treated with TL (A, C, E) or CM (B, D, F) and HA (LMW and HMW). Data are expressed as normalized relative quantities (NRQ) mean ± SEM, from four independent experiments. \* $P < 0.05$ , \*\* $P < 0.01$ , and \*\*\* $P < 0.001$ , one-way ANOVA analysis.

MØ cells, we examined the effect of TL or CM with or without HA addition on their mRNA expression levels. The treatment with HWM HA induces an increase in CD44 expression levels (NRQ:  $1.676 \pm 0.3466$ ) with respect to BC (NRQ:  $1.107 \pm 0.1700$ ), but has no significant effect on TLR-4 or RHAMM expression levels (Fig. 6A,C,E). Besides, MTL plus HMW HA significantly decreased the expression levels of CD44 (NRQ:  $0.5866 \pm 0.02388$ ) and TLR4 (NRQ:  $0.4602 \pm 0.1234$ ), in comparison to the treatment of MTL without HA (NRQ:  $2.043 \pm 0.4256$ ), without modulating RHAMM expression levels (Fig. 6A,C,E). In contrast, no differences were observed among the LTL treatments (Fig. 6A,C,E). We also evaluated the behavior of Mo/MØ cells exposed to CM from tumor-living cells. These CM did not affect CD44, TLR-4, and RHAMM expression levels (Fig. 6B,D,F). However, MCM plus HMW HA significantly decreased TLR-4 expression levels (NRQ:  $0.7250 \pm 0.01500$ ) in comparison to MCM without HA treatment (NRQ:  $1.635 \pm 0.03500$ ) (Fig. 6D). CD44 and RHAMM levels showed no difference between MCM treatments (Fig. 6F). As for LCM treatments, no differences were observed among them in the expression levels of the receptors analyzed (Fig. 6B,D,F).

#### Mo/MØ preincubated with HMW HA increased the tumor vasculature in the breast cancer model

We tested whether the *in vitro* angiogenic effects could be observed in an *in vivo* model. For this purpose, nude mice were injected with MDA-MB-231 or Lovo cells, and 9 days later, animals with similar tumor volume were inoculated with Mo/MØ preincubated with HMW or LMW HA. Tumor volume was measured weekly and we found no differences in tumor growth between treatments (data not shown). Tumors were fixed and sections were stained with: (a) H&E to rule out changes in tumor histology or (b) GSL-1 to analyze ECs forming blood vessel.

We observed that Mo/MØ preincubated with HMW induced a significant increment of the tumor vasculature in the MDA-MB-231 model detected by immunofluorescence intensity (AU) of GSL-1-FITC (AU:  $1.759 \pm 0.1173$ ) compare to Mo/MØ without treatment (AU:  $1.158 \pm 0.1193$ ) and pulsed with LMW HA (AU:  $1.017 \pm 0.07250$ ) (Fig. 7A). Besides, the tumor vasculature decreased in those animals inoculated with Mo/MØ previously treated with LMW HA in comparison with tumor control (AU:  $1.602 \pm 0.1307$ ) (Fig. 7A). However, in LoVo model, we observed no difference in the vasculature after all treatments (Fig. 7B). Tissues section for each model

and treatments presented similar tumor structure without necrosis areas. In conclusion, *in vivo* data confirm and are in concordance with the *in vitro* results.

#### TSG-6 production by Mo/MØ is deregulated with HMW HA in a breast carcinoma microenvironment

Taking into account the results presented above, we could indicate that there is a factor whose expression in Mo/MØ is triggered by HMW HA in breast carcinoma context but not in colorectal. Therefore, we decided to evaluate gene and protein expression levels of TSG-6, a HA-binding protein, that modulates its structure and function in inflammatory or tissue injury process [5,24]. Firstly, GEO2R was applied to screen TSG-6 expressed mRNA levels in macrophages. TSG-6 was screened in two mice datasets: breast (GSE18404) and colorectal (GSE67953) carcinoma; TSG-6 was expressed in both datasets, but no differences were found between TAMs and spleen macrophages (Fig. 8). We observed that TSG-6 mRNA expression levels were not modulated significantly in Mo/MØ treated with LMW or HMW HA. However, we found different TSG-6 expression levels when Mo/MØ were pulsed with MTL (NRQ:  $5.860 \pm 2.711$ ) compared to BC (NRQ:  $0.3615 \pm 0.1206$ ) and LTL (NRQ:  $1.233 \pm 0.4856$ ) (Fig. 9A). Besides, TSG-6 mRNA levels decreased in Mo/MØ treated with MTL plus HMW HA (NRQ:  $0.4540 \pm 0.1535$ ) in comparison to MTL without HA (NRQ: NRQ:  $5.860 \pm 2.711$ ). However, Mo/MØ pulsed with LTL, with or without HA, showed no differences in TSG-6 mRNA levels (Fig. 9A). In the case of CM treatments, MCM plus HMW HA significantly increased TSG-6 mRNA levels (NRQ:  $18.35 \pm 4.835$ ) when compared to MCM treatment without HA (NRQ:  $3.703 \pm 1.603$ ) (Fig. 9C).

In addition, we analyzed TSG-6 protein expression through western blot in Mo/MØ supernatants and we detected two species: (a) ~ 35 kDa corresponding to free TSG-6 and (b) ~ 120 kDa corresponding to the complex generated by the heavy chain (HC) of I $\alpha$ I and TSG-6, as have been documented by other authors [25]. We found that, in Mo/MØ supernatants, free TSG-6 was increased with MTL treatment (AU:  $24.73 \pm 3.472$ ) or LTL treatment (AU:  $19.78 \pm 2.301$ ) with respect to BC (AU:  $2.773 \pm 1.337$ ) (Fig. 9B). MTL plus HMW HA diminished the 120 kDa species, when compared to MTL (AU:  $10.69 \pm 1.297$ ). LTL plus HMW HA ( $10.69 \pm 1.297$  AU) diminished the 120 kDa species, when compared LTL ( $11.56 \pm 1.054$  AU) without HA treatment (Fig. 9B).

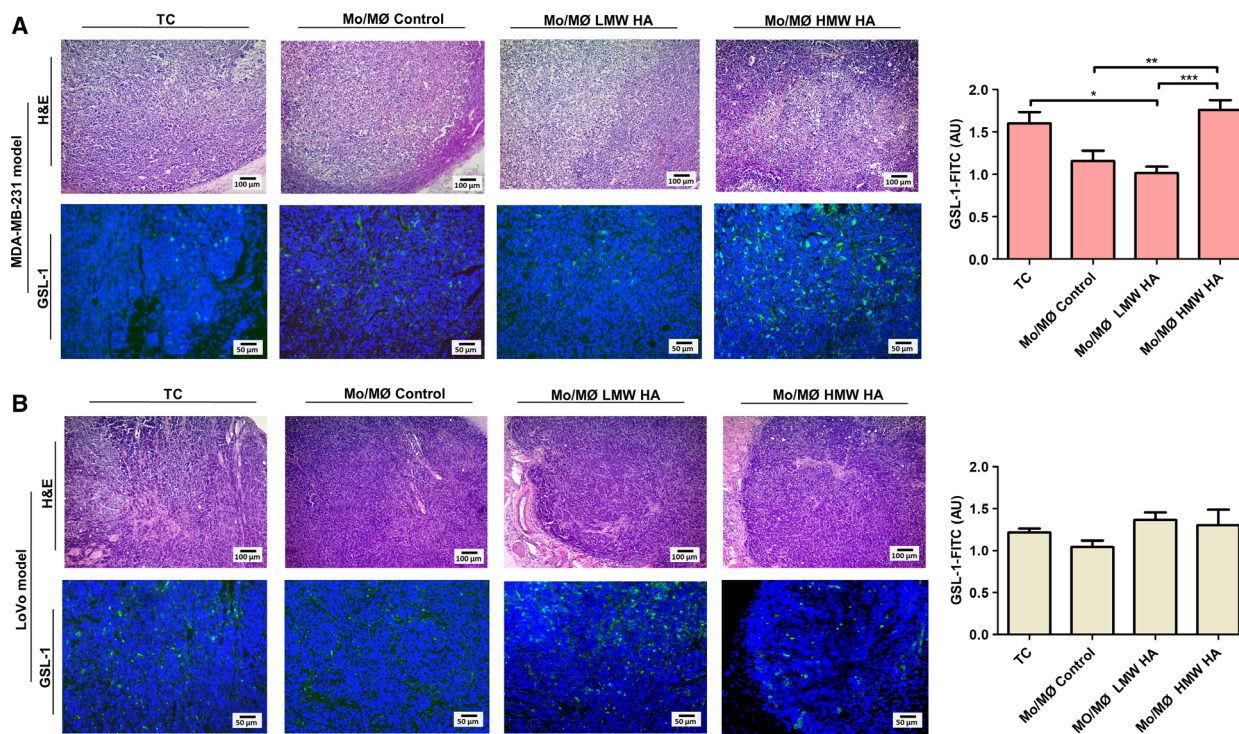


**Fig. 7.** *In vivo* angiogenesis in cancer xenograft model. (A) MDA-MB-231 model and (B) LoVo model. H&E: tumors were fixed and stained with hematoxylin/eosin. GSL-1: quantification of GSL-1-FITC (binds specifically to endothelial cells) by fluorescence microscopy in tumor sections of breast cancer xenograft model. Nude mice were inoculated with MDA-MB 231 or LoVo and at day 9, tumors with a similar volume were inoculated with Mo/MØ previously treated or not with LMW or HMW HA. Tumors were fixed and stained with GSL1-FITC (green, endothelial cells) and DAPI (blue, nuclei). Bars represent the average of GSL-1-FITC+/field  $\pm$  SEM from 10 representative visual fields. \* $P < 0.05$ , \*\* $P < 0.01$ , and \*\*\* $P < 0.001$ , one-way ANOVA analysis. TC, tumor control.

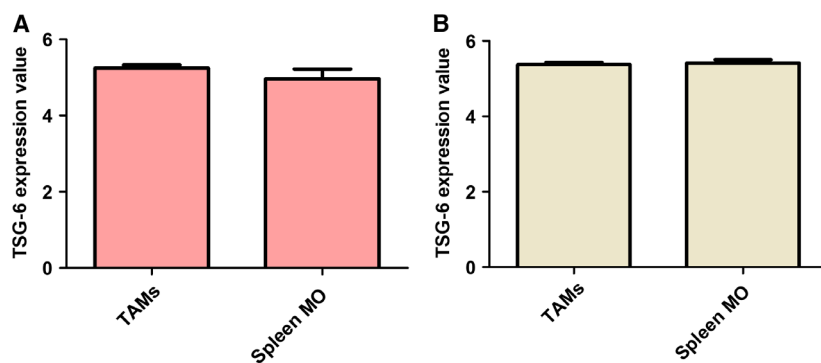


**Fig. 8.** Microarray datasets. (A) GSE18404 (breast carcinoma) and (B) GSE67953 (colorectal carcinoma) were used for comparing differential TSG-6 expression levels in TAMs and spleen MO. In each dataset, NCBI GEO2R tool was used to analyze TSG-6 levels.

We also performed TSG-6 western blot from Mo/MØ supernatants treated with MCM or LCM (Fig. 9D). MCM plus HMW HA increased  $\sim 35$  kDa species corresponding to free TSG-6 (AU:  $9.755 \pm 0.07500$ ) with respect to MCM (AU:  $4.675 \pm 0.3850$ ) and BC (AU:  $2.773 \pm 1.337$ ) (Fig. 9D). However, the  $\sim 120$  kDa species, corresponding to TSG-6-HC, significantly decreased with MCM plus HMW HA (AU:  $5.347 \pm 1.509$ ) when compared to MCM without HA (AU:  $10.78 \pm 2.289$ ).

This species corresponding to TSG-6-HC was not detected in the supernatants of Mo/MØ treated with LCM with or without HA (Fig. 9D right panel).

#### Mo/MØ preincubated with HMW HA decreased TSG-6 levels in breast cancer model

In order to evaluate the intrinsic effects of these molecules in the tumor stroma, tumor sections of xenograft models were stained with TSG-6 and HA by

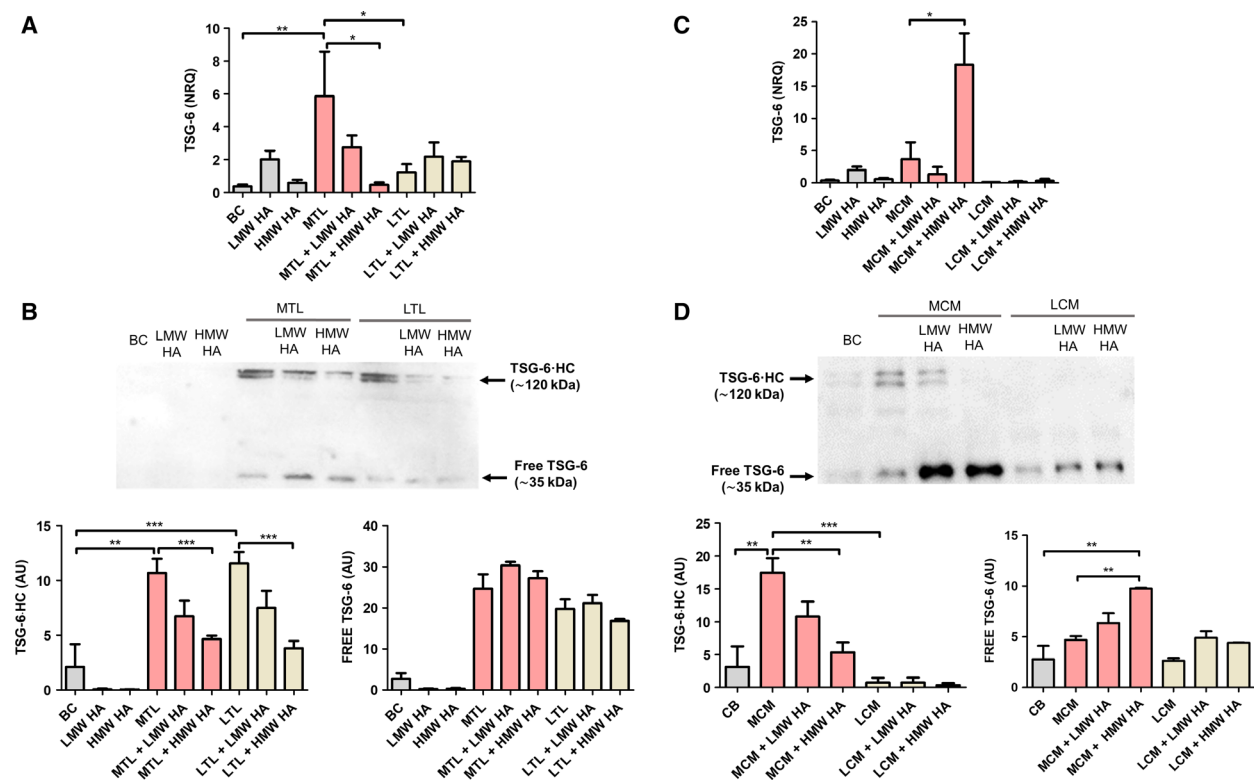


**Fig. 9.** TSG-6 mRNA and protein levels in Mo/MØ treated with HA. (A and C) TSG-6 mRNA expression levels were measured by RT-qPCR in Mo/MØ treated with TL (A) or CM (C) and HA (LWW and HMW). Data are expressed as normalized relative quantities (NRQ) mean  $\pm$  SEM, from three independent experiments. (B, D) TSG-6 protein levels were measured by western blot in Mo/MØ supernatants MØ treated with TL (B) or CM (D) and HA (LWW and HMW). TSG-6-HC (~120 kDa) right panel; free TSG-6 (~35 kDa) left panel. Protein levels were quantified by densitometry from four independent experiments. \* $P < 0.05$ , \*\* $P < 0.01$ , and \*\*\* $P < 0.001$ , one-way ANOVA analysis.

immunofluorescence. In the MDA-MB-231 model, mice inoculated with Mo/MØ without treatment (AU:  $3.201 \pm 0.3712$ ) increased TSG-6 levels respect to control mice (without inoculation of Mo/MØ) (AU:  $1.624 \pm 0.1989$ ) (Fig. 10A). Besides, mice inoculated with Mo/MØ preincubated with HMW HA, which presented a significant increment of the tumor vasculature, decreased TSG-6 immunofluorescence intensity (AU:  $1.820 \pm 0.4308$ ) when compared to mice inoculated with Mo/MØ without treatment (AU:  $3.201 \pm 0.3712$ ) (Fig. 10A). In contrast, TSG-6 levels in the LoVo model presented no differences among treatments (Fig. 10B). These TSG-6 results from the *in vivo* model are in concordance with the *in vitro* results obtained for TSG-6 mRNA levels (Fig. 9A). When we analyzed total endogenous HA levels, we found no significant differences in the MDA-MB-231 model. Contrary, tumor sections derived from mice of the LoVo model inoculated with Mo/MØ preincubated with HMW HA, presented a significant increment in total HA (Fig. 10B). Thus, despite similar or dissimilar

accumulation of HA in the tumor is the differential expression of TSG-6 that might affect HA action in Mo/MØ within both tumor models, which also affect their angiogenic behavior.

### TSG-6 levels were deregulated when Mo/MØ derived from cancer patients were treated with HMW HA and tumor tissue lysates

To further evaluate HA effect on human Mo/MØ angiogenic behavior, we used Mo/MØ derived from cancer patients (breast and colorectal) and we prepared from each patient lysate from tumor tissue (TTL) and from normal tissue adjacent to the tumor (NATL). In Mo/MØ samples derived from breast cancer patients (ER-positive), free TSG-6 protein levels (~35 kDa species) increased with TTL treatment plus HMW HA (AU:  $19.94 \pm 0.7000$ ) respect to TTL without HA (AU:  $7.485 \pm 2.045$ ) (Fig. 11A, right panel). Free TSG-6 levels did not show significant differences among NATL treatments (Fig. 11B, right panel). As

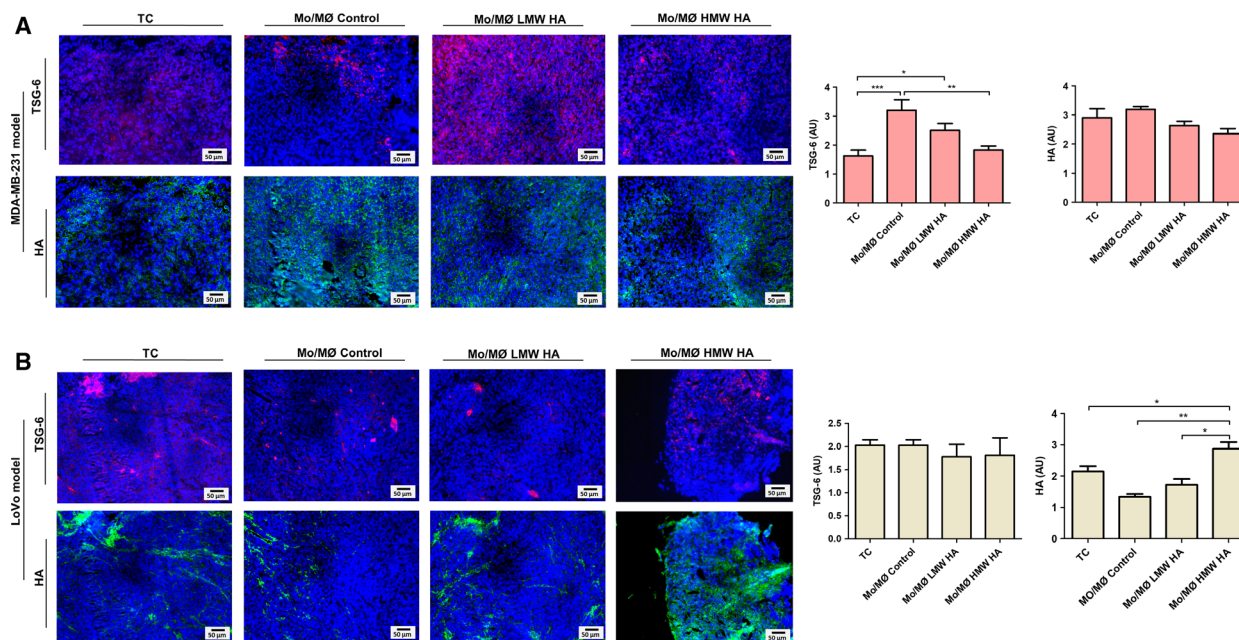


**Fig. 10.** TSG-6 and HA immunostaining in cancer xenograft model. (A) MDA-MB-231 model, (B) LoVo model. Tumor sections were stained with TSG6 and anti-rabbit conjugated with Texas Red (red, TSG-6); HA-binding protein biotinylated and streptavidin-FITC (green, total HA); and DAPI (blue, nuclei). Bars represent the average of TSG-6+ or HA+/field  $\pm$  SEM from 10 representative visual fields. \* $P < 0.05$ , \*\* $P < 0.01$ , and \*\*\* $P < 0.001$ , one-way ANOVA analysis. TC, tumor control.

for TSG-6-HC (~120 kDa species), it showed a decrease when Mo/MØ were treated with breast TTL plus HMW HA (AU:  $6.215 \pm 1.225$ ) in comparison to TTL (AU:  $16.34 \pm 2.095$ ) (Fig. 11A, left panel), but among NATL treatments, we did not observe significant differences (Fig. 11B, left panel). Mo/MØ samples derived from colorectal carcinoma showed no significant differences between TTL and NATL treatments.

## Discussion

Macrophages derived from monocytes exhibit a diversity cell behavior, beyond its immunological role. These cells secrete crucial factors for growth and remodeling of the microvasculature during angiogenesis. Despite vast investigations of Mo/MØ response to tumor cells and inducers of angiogenesis, few studies are focused on evaluating their behavior considering the extracellular matrix interaction. This issue is an important point of study to develop novel cancer therapies that target angiogenesis and simultaneously immunosuppression. For example, it has been demonstrated that disruption of angiogenesis substantially enhances the efficacy of immune-based cancer therapies [26].

As mentioned previously, HA is one of the extracellular matrix components that can modify the behavior

of both tumor and immune cell types [1]. HA interacts with Mo/MØ inducing their migration, the release of chemokines, cytokines, growth factors, and expression of MMPs [27]. However, it has been observed that HA released by tumor cells selectively deactivate Mo/MØ inhibiting their antitumor immune response [28,29]. Recent works showed that HA derived from breast cancer induces MØ to acquire an immunosuppressive or M2-like phenotype [30]. It is well established that HA size is critical for its function. Thus, we used LMW HA and HMW HA of defined size in our experiments. We observed that HA, both as LMW or HMW, in the presence of tumor factors, either from tumor lysates or conditioned media from breast (MTL) or colorectal (LTL) cells, did not affect surface markers that define the MØ phenotype [31]. Besides, it is important to consider that Mo/MØ behavior and function is not only defined by cell surface markers, and a better characterization may also be possible *in vivo* based on the paracrine factors that they secrete.

To evaluate Mo/MØ as an inducer of angiogenesis under HA treatments in a tumor context, we analyzed the expression of biosynthesis of VEGF, the main angiogenic factors (Fig. 3A,B). We evaluated Mo/MØ behavior between the different tumor types and exposing them to tumor cells lysates (TL) or soluble factors from tumor cells conditioned media cells (CM).

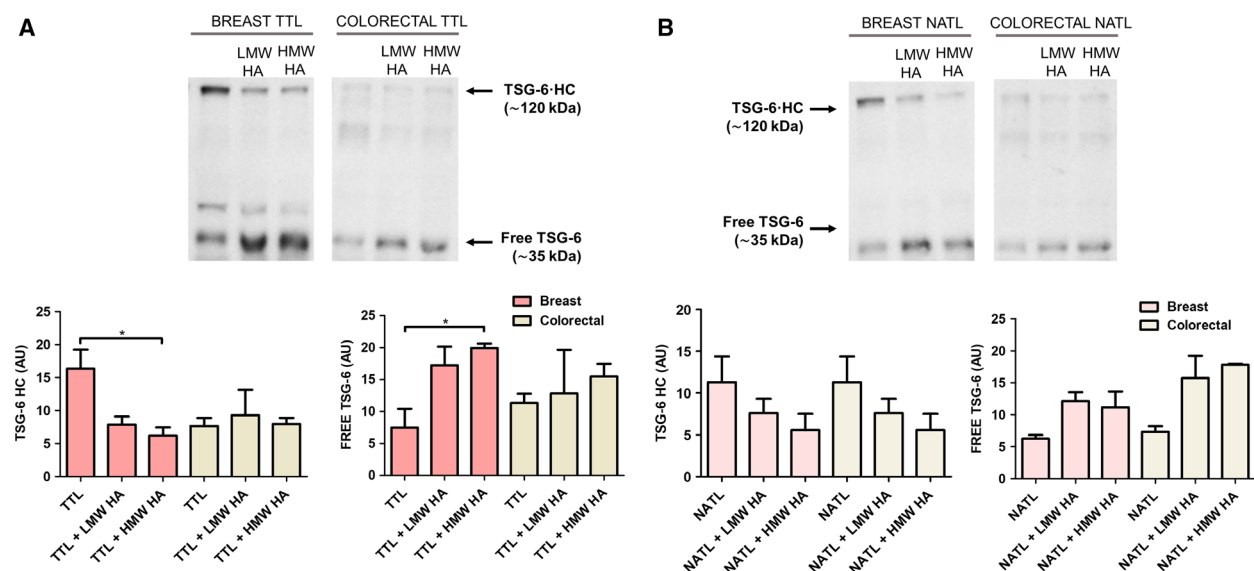


**Fig. 11.** TSG-6 protein levels in Mo/MØ treated with HA derived from patients (breast and colorectal cancer). (A) TSG-6 protein levels were measured by western blot in Mo/MØ supernatants MØ treated with TL derived from breast or colorectal tumor tissue and HA (LMW and HMW). (B) TSG-6 protein levels were measured by western blot in Mo/MØ supernatants MØ treated with NATL derived from breast or colorectal normal tissue adjacent to the tumor. TSG-6-HC (~120 kDa) right panel; free TSG-6 (~35 kDa) left panel. Protein levels were quantified by densitometry and expressed as arbitrary units (AU) mean  $\pm$  SEM, from four independent experiments. \* $P < 0.05$ , one-way ANOVA analysis.

These cells need to be stimulated to produce VEGF and HA by itself was not able to induce this expression. Even more, HMW HA but only in the presence of breast carcinoma antigens (MTL or MCM) increased significantly VEGF mRNA levels (Fig. 3A, B). Similar results were observed when we evaluated other pro-angiogenic molecules like IL-8 and FGF-2 (Fig. 1C–F) [32]. Thus, it is possible to hypostatize that there are different factors in the tumor lysates or conditioned media from breast cancer cells, but not in colorectal cancer cells, that could be modulating the function of HWM HA on Mo/MØ. Besides, we found a significant increase in MMP-2 gelatinolytic activity when Mo/MØ were treated with HA (LMW or HMW) in the presence of MTL (Fig. 4C). However, mRNA MMP-2 levels increased only during the treatment with MTL plus HMW HA (Fig. 4D). It was documented that MMP-2 cleaves collagen type IV and it is associated with ECs migration, affecting their capacity to generate new vessel [33]. Besides, it was previously demonstrated that HA-CD44 interaction allows the activation of MMP-2 [34]. Thus, factors that modulate HA function might be directly connected with the MMP-2 activity, since we observed a modulation with MTL but not with LTL treatment. To further study the biological function of angiogenic factors released with the different treatments, we analyzed the migration capability of ECs toward the Mo/

MØ supernatants. A higher migration was observed with MTL and even more with MTL plus HMW HA treatment (Fig. 5), suggesting that factors in MTL induce an HA with pro-angiogenic action on Mo/MØ. In turn, these cells release VEGF, IL-8, FGF-2, and MMP-2 that stimulate ECs migration. Similar results were observed when we evaluated angiogenesis *in vivo* analyzing the vessels by the detection of ECs. We found a significant increase in ECs staining in tumor tissue of MDA-MB-231-bearing mice that were treated with MØ primed with HMW HA, but no differences were detected in LoVo-bearing mice (Fig. 7).

To study HA receptors that are involved in the Mo/MØ responses, we evaluated CD44, TLR-4, and RHAMM mRNA expression levels (Fig. 6). It has been shown that CD44 and TLR-4 are involved in immune deactivation of human Mo/MØ cells [23]. Actually the modulation of this receptor's expression affects their immune phenotype and function within the tumor microenvironment [1]. We only observed the modulation of these receptors in Mo/MØ exposed to treatments with antigens from breast cancer cells lines. We observed that HMW HA treatment induced a significant downregulation of CD44 and TLR-4 expression in Mo/MØ in the presence of MTL; for TLR-4, we also observed a significant decrease in MCM plus HMW HA. Thus, the decrease in HA receptor expression could be associated with angiogenesis and

involved in HA response *in vivo* according to the type of tumor microenvironment. In light of these results, we carried out subsequent experiments to identify the factor/factors that is/are modulating the HA function and in turn Mo/MØ angiogenic behavior in both types of cancer. Although HA is not covalently linked to a core protein, it can interact with HA-binding proteins or hyaladherins, that in turn modulate HA structure and function. TSG-6, is a well-characterized hyaladherin, with an HA-binding site located within a domain called 'link module' [18,24]. For example, it has been observed that aggregation of HA IαI-induced is dependent on TSG-6 and allows the stabilization of the extracellular matrix [24]. Thus, alteration of TSG-6 might affect HA function. We suggest that the differences found in Mo/MØ behavior when they were exposed to different sizes of HA and different tumor types could be associated with HA-binding proteins that in turn modulate HA action. In most cell types, the expression of TSG-6, as immunoregulator mediator, is stimulated by cytokines or factors released during inflammation, inflammation-like, or injury processes. It is proposed that TSG-6 controls inflammation response and maintains the extracellular matrix homeostasis [18].

For the first time, we detected a reduction in the expression levels of the bands corresponding to the complex TSG-6-HC only when Mo/MØ were treated with HA (HMW or LMW) plus MTL, LTL, or MCM. Markedly, TSG-6-HC protein expression was only modulated in breast tumor context. Indicating that specific tumor factors could induce an immunosuppressive and angiogenic action of TAMs by modulating TSG-6, and its expression within the tumor is also modulated by the interaction with extracellular matrix components such as HA. The TSG-6-HC complex is indicative of the enzymatic activity of TSG-6. It is well known that TSG-6 catalyzes the transfer of the IαI HC to HA, affecting the activity of this proteinase inhibitor [3,4] as well as HA structure, the binding capacity to its receptors and therefore its function [24].

Even more, we used xenograft nude mice models, which do not allow the development of adaptive immune response, but innate immune response is still intact and offers a tumor milieu to study Mo/MØ function and regulation of angiogenesis. We observed that the treatment of Mo/MØ induced an increase in TSG-6 that was significantly reduced during the treatment of Mo/MØ preincubated with LMW HA in breast carcinoma model (Fig. 10A). These results are in agreement with *in vitro* results where TSG-6 mRNA levels decreased in Mo/MØ treated with MTL plus HMW HA in comparison to MTL without HA. When HA expression was analyzed in tumor tissues, no

changes were detected in the breast carcinoma model. This indicates that different function of HA is dependent on factors or antigens of the tumor microenvironments than the amount of HA present within the tissues. The analysis of Mo/MØ treated with tumor or normal adjacent tissue derived from patients with invasive breast carcinoma (ER+, stage I or II) or colorectal carcinoma (stage I or II) allowed us to extend our results in the context of different types and stages of breast and colorectal carcinoma. Mo/MØ cells treated with TTL from breast cancer patients plus HMW HA also modulate both species of TSG-6 (HC bonded and free). Besides, no modulations were observed from colorectal cancer and normal tissues. Considering our results, we can conclude that the modulation of TSG-6 activity and expression is differentially modulated according to tumor type. However, further studies will be necessary to find the factors present in breast carcinoma that are involved in this HA-TSG-6 regulation loop.

As for Mo/MØ treated with colorectal carcinoma antigens, HMW HA did not affect HA receptors, TSG-6 nor their angiogenic behavior. Interestingly, the role of macrophages in colorectal carcinoma is controversial. Some studies support that TAMs exhibit tumor-suppressive abilities, whereas others report that these cells contribute to colorectal cancer promotion [35]. However, it was shown that high density of tumor-associated MØ correlates with poor prognosis in breast carcinoma since this cells were capable of inducing angiogenesis, remodeling the tumor extracellular matrix to aid invasion, modeling breast cancer cells to evade host immune system and recruiting immunosuppressive leukocytes to the tumor microenvironment [36].

Finally, this study showed for the first time that HMW HA, a highly conserved and poorly immunogenic molecule, downregulates TSG-6 levels in Mo/MØ modulating their angiogenic behavior in breast carcinoma milieu, but not in colorectal carcinoma. Even more, CM-induced downregulation of TSG-6-HC complex could be essential for *in vivo* angiogenesis because this effect was not observed in LCM. These findings are of great interest, since it may provide novel breast cancer targets, especially to increase the success of anti-angiogenic agents.

## Materials and methods

### Reagents

Pharmaceutical endotoxin-free HA recombinant of definite size: HMW 1.5–1.8 × 10<sup>6</sup> Da and LMW 1–3 × 10<sup>5</sup> Da from CPN spol.s.r.o was kindly supplied by Farma-trade (Villa Lynch, Bs As., Argentina).

## Cell lines and human blood

LoVo (human colorectal adenocarcinoma) provided by L. Policastro (Instituto de Nanociencia y Nanotecnología, BA, Argentina) and MDA-MB-231 (breast adenocarcinoma) by Roxana Schillaci (IBYME, CABA, Argentina) were maintained with DMEM/F12 supplemented with 10% FBS, 2 mM L-glutamine, 100 U·mL<sup>-1</sup> streptomycin, and 100 mg·mL<sup>-1</sup> penicillin and incubated at 37 °C in a 5% CO<sub>2</sub> humidified atmosphere. HMEC-1 (dermal microvascular endothelium) cell line was cultured with DMEM supplemented with 10% FBS, 2 mM L-glutamine, 100 U·mL<sup>-1</sup> streptomycin, and 100 mg·mL<sup>-1</sup> penicillin and incubated at 37 °C in a 5% CO<sub>2</sub> humidified atmosphere. In all cell cultures, periodic checkups of cell morphology were performed as well as strict control of cell line passages (5–10th passage) and cell line growth rate. In addition, all cell lines were analyzed to discard the presence of mycoplasma contamination by PCR assay.

Peripheral blood samples for human monocyte isolation were obtained from voluntary blood donors and from cancer patients. Tumor tissue as well as normal tissue adjacent to the tumor (NAT) was obtained from cancer patients. Approval was obtained from the Institutional Assessment Committee (CIE)—IRB within the Austral University Hospital (CIE N° 17-006). Informed consent was obtained from participants in accordance with the Declaration of Helsinki.

## Tumor lysates and conditioned media

Confluent cultures of LoVo or MDA-MB-231 cells were detached with cold PBS, washed twice in PBS, and resuspended in PBS. Cell suspensions ( $1.2 \times 10^6$  cells·mL<sup>-1</sup>) and conditioned media (CM) were frozen at -80 °C. The cell suspensions were disrupted by five freeze–thaw cycles. To remove large debris, tumor lysates (TL) MDA-MB-231 (MTL) or LoVo (LTL) were centrifuged at 300 r.p.m. for 10 min. The supernatant was collected and passed through a 0.22 mm filter unit. Conditioned media (CM) were collected from supernatants from tumor cell lines MDA-MB-231 (MCM) or LoVo (LCM) cultured ( $1.2 \times 10^6$  cells) for 6 h without serum. The protein concentration was determined by Bradford assay. Cancer patient's lysates were prepared using the same protocol as for tumor cells lysates with previous mechanical disintegration of the tissues. Lysates derived from tumor tissue (TTL) and from normal tissue adjacent to the tumor (TNAT). The resulting TL or CM was aliquoted and stored at -80 °C until use.

## Isolation of PBMC-derived Mo/MØ

Peripheral blood mononuclear cells were isolated by the Ficoll-Paque Plus (GE Healthcare Bio-Sciences AB, Uppsala, Sweden) gradient. Cells were plated into 12-well plates for 2 h, removing the non-adherent cells. Then, adhered

cells were subsequently cultured overnight in complete RPMI 1640 medium [37]. Twenty-four hours later, the medium of the adherent MØ was replaced with RPMI 1640 (FBS free) and were pulsed with either with conditioned media or TL ( $200 \mu\text{g}/10^6$  cells·mL<sup>-1</sup>) with or without LMW HA ( $20 \mu\text{g}\cdot\text{mL}^{-1}$ ) or HMW HA ( $20 \mu\text{g}\cdot\text{mL}^{-1}$ ). After 24 h, cells were centrifuged, characterized by flow cytometry, and used for experiments.

## MTS

Cell viability assay was measured by MTS method (ab197010; Abcam, Cambridge, UK) as described in the manufacturer protocol. Mo/MØ treated with MTL or LTL (0, 100, 200, and 400  $\mu\text{g}\cdot\text{mL}^{-1}$ ) were seeded in 96-well plates at a density of  $6 \times 10^3$  per well, and 3 h before the treatments ended, the MTS dye was added and then incubated for 3 h in the dark. The optical density (OD) values were measured at 490 nm.

## Flow cytometry analyses

Staining and flow cytometric analyses of PBMC-derived MØ were carried out using standard procedures. Briefly,  $10^6$  cells were blocked with PBS-1% BSA for 45' and then were stained on ice for 30 min with different conjugated antibodies: anti-CD14; anti-MHC-II (G46-6); anti-CD80 (L307.4); and anti-CD206 (all from BD Biosciences, San Jose, CA, USA). Cells were washed thoroughly with PBS-1% BSA and subjected to flow cytometry (FACS CANTO II-BD, Becton Dickinson and Company, Franklin Lakes, NJ, USA). Data were analyzed using FLOW 7.6.2 software (Becton Dickinson and Company).

## ELISA assays

VEGF expression levels were determined by a sandwich ELISA assay (DY293B; R&D Systems, Inc., Minneapolis, MN, USA) from free-cell conditioned media. The assays were carried out according to the instructions provided by the manufacturer.

## RT-qPCR

Total RNA was extracted by Tri Reagent (TR 118; Molecular Research Center, Inc., Ohio, USA). RNA quantification was evaluated by spectrophotometry. Then, 2  $\mu\text{g}$  of RNA was reverse transcribed with 200U RT M-MLV Reverse Transcriptase (M1701; Promega, Fitchburg, WI, USA) and 2.5 pmol· $\mu\text{L}^{-1}$  of Oligo (dT) primers (GenBiotech, CABA, Argentina). cDNAs were then subjected to real-time quantitative PCR (RT-qPCR) using FastStart SYBR Green Master (04673484001; Roche, Mannheim, Germany) and 200 nm of each specific primer (Invitrogen, Life Technologies™, Carlsbad, CA, USA):

- IL-8: forward 5'-AAGGAAACTGGGTGCAGAG-3' and reverse 5'-GGCATCTTCACTGATTCTTG-3'
- FGF-2: forward 5'-CCTGGCTATGAAGGAAGATGG-3' and reverse 5'-TCGTTTCAGTGCCACATACC-3'
- TSG-6: forward 5'-CATATGGCTTGAACGAGCAGC-3' and reverse 5'-CTTTGCGTGTGGGTTGTAGC-3'
- RHAMM: forward 5'-TGGAAAAGATGGAAGCAAGG-3' and reverse 5'-CCAGTGTAGCATTATTCGAGAG-3'
- CD44: forward 5'-GTGATGGCACCCGCTATG-3' and reverse 5'-ACTGTCTTCGCTCTGGGATGG-3'
- TLR4: forward 5'-TGAGCAGTCGTGCTGGTATC-3' and reverse 5'-CAGGGCTTTTCTTGAGTCTGTC-3'
- GAPDH: forward 5'-GGGGCTGCCAGAACATCAT-3' and reverse 5'-GCCTGCTTACCACCTTCTTG-3'

PCR conditions were: 90 s at 94 °C and then 40 cycles of 30 s at 94 °C, 30 s at 60 °C, and 30 s at 72 °C. Values were normalized to the levels of GAPDH housekeeping gene.

### Western blot

To analyze TSG-6 biosynthesis in MØ supernatants, equal amounts of protein were resolved by 0.1% SDS-10% polyacrylamide gel denaturing electrophoresis (SDS/PAGE) and transferred to a nitrocellulose membrane. The membranes were incubated overnight at 4 °C with RAH-1 a polyclonal human TSG-6 antibody [38] (kindly supplied by A. Day) and then incubated for 1 h at RT with horseradish peroxidase-labeled secondary antibody. Finally, HRP chemiluminescence reaction was detected using a stable peroxide solution and an enhanced luminol solution. Images were obtained with ImageQuant 4000 mini bioluminescent image analyzer (GE Healthcare LifeSciences) and analyzed using IMAGEJ (National Institutes of Health, Bethesda, MD, USA).

### Gelatin zymography

Matrix metalloproteinases (MMPs) activity in MØ supernatants was determined by gelatin zymography [39]. Conditioned media were run on a 10% SDS/PAGE containing 0.1% gelatin (Sigma-Aldrich, St. Louis, MO, USA). Following electrophoresis, gels were washed with 50 mM Tris-CIH pH 7.5, 2.5% Triton X-100 30 min, 50 mM Tris-CIH pH 7.5, 2.5% Triton X-100, 5 mM CaCl<sub>2</sub>, 1 mM ZnCl<sub>2</sub> 30 min and 50 mM Tris-CIH pH 7.5, 2.5% Triton X-100, 10 mM CaCl<sub>2</sub>, 200 mM NaCl 48 h at 37 °C. The gel was stained with Coomassie Brilliant Blue R-250 for 30 min at room temperature. Gelatinase activity was visualized by negative staining; gel images were obtained with a

biomolecular imager (ImageQuant LAS 4000 mini, GE Healthcare Bio-Sciences AB, Uppsala, Sweden) and were subjected to densitometric analysis using IMAGEJ 1.50b software package (National Institutes of Health, Bethesda, MD, USA). Fold change MMP-2 and MMP-9 activity was obtained by normalizing values to untreated samples.

### *In vitro* endothelial cell migration assay

*In vitro* migration was performed using a 48-Transwell microchemotaxis Boyden Chamber unit (Neuroprobe, Inc., Gaithersburg, MD, USA). HMEC-1 ( $1.5 \times 10^3$  cells/well) was placed in the upper chamber and conditioned medium of the treatments was applied to the lower chamber of the transwell unit. As a negative control, cells were exposed to DMEM and RPMI without FBS, and as a positive control, a medium rich in angiogenic factors was used. The chamber was left for 4 h at 37 °C in a 5% CO<sub>2</sub> humidified atmosphere. Cells attached to the lower side of the membrane were fixed in 2% formaldehyde and stained with 4',6-diamidino-2-phenylindole dihydrochloride (DAPI; Sigma-Aldrich). Images from three representative visual fields were captured using Nikon Eclipse E800 fluorescence microscope and were analyzed using CELLPROFILER software (www.cellprofiler.org), and the mean number of cells/field  $\pm$  SEM was calculated.

### Tumor xenograft model

Six- to eight-week-old male nu/nu mice were purchased from Comisión Nacional de Energía Atómica, Ezeiza, Buenos Aires, Argentina. Animals were maintained at our Animal Resources Facilities (CIBA, CIT NOBA) in accordance with the experimental ethical committee and with the NIH Guide for the Care and Use of Laboratory Animals (eighth edition). MDA-MB-231 or LoVo cell suspension ( $1 \times 10^7$  cells/0.1 mL) was injected subcutaneously in the dorsal flank of mice. After 9 days, PBMC-derived Mo/MØ treated or not with LMW or HMW HA were inoculated subcutaneously near the base of the tumor. On day 29, mice were sacrificed and tumors were removed, fixed in 10% formalin, and embedded in paraffin. Before staining, 3- $\mu$ m sections were deparaffinized and dehydrated.

### Detection of angiogenesis in tumor tissues

Slides were rinsed with PBS and dye with DAPI 0.3  $\mu$ g-mL<sup>-1</sup> plus fluorescein-labeled Griffonia (Bandeiraea) Simplicifolia Lectin I 20  $\mu$ g-mL<sup>-1</sup> (GSL I; FL-1101; Vector Laboratories, Burlingame, CA, USA) that binds specifically to endothelial cells in mouse tissues [40]. The sections were rinsed with PBS and then mounted on microscope slides. Images of the stained sections were taken with a Nikon Eclipse E800 fluorescence microscope (Nikon Instruments Inc., Melville, NY, USA). Microvessels were quantified with IMAGEJ.

## Immunostaining of TSG-6 and HA in tumor tissues

Slides were rinsed with PBS and incubated overnight at 4 °C with rabbit anti-human polyclonal against TSG-6 (RAH-1) [38] and HA-binding protein (385911; EMD Millipore Corp., Merck KGaA, Darmstadt, Germany). Afterward, the tissue slices were washed three times in PBS and then incubated for 1 h at 4 °C with secondary rabbit antibody conjugated with Texas Red® (TI-1000; Vector Laboratories) and streptavidin conjugated with FITC (31274243; Immunotools, Friesoythe, Germany). The sections were rinsed with PBS, dye with DAPI 0.3 µg·mL<sup>-1</sup> and then mounted on microscope slides. Images of the stained sections were taken with a Nikon Eclipse E800 fluorescence microscope and quantified with IMAGEJ.

## Microarray datasets processing

Publicly available mice microarray datasets GSE18404 (breast carcinoma) and GSE67953 (colorectal carcinoma) were used for comparing differential TSG-6 expression levels in TAMs and spleen MO. In each dataset, NCBI GEO2R tool (<http://www.ncbi.nlm.nih.gov/geo/geo2r/>) was used to analyze TSG-6 mRNA expression levels.

## Statistical analysis

For statistical analysis, 95% confidence intervals (CI) were determined by calculating arithmetic mean values and variance (standard deviation, SD) of three independent experiments. To evaluate whether differences between the values obtained were significant, analysis of variance (ANOVA, Tukey test) was used to evaluate the differences between values of more than two experimental groups. The software PRISM (GraphPad, San Diego, CA, USA) was used, considering a *P* value < 0.05 as statistically significant.

## Acknowledgements

We thank Natalia Menite for technical assistance in flow cytometry and Gaston Villafañe for laboratory animal assistance from Centro de Investigaciones Básicas y Aplicadas (UNNOBA); biochemist Lucia Romano, as support staff for research and development from CIT NOBA, for technical assistance in immunohistochemistry analysis; Daniel Petraglia for technical assistance in histopathological analyzes; the surgery service of the Clínica Centro; the gynecology (C. Lopez, MD and L. Walker, MD), pathology, and surgery service and the clinical analysis laboratory from Hospital Interzonal General de Agudos Abraham F. Piñeyro; and Anthony Day for providing the TSG-6 primers sequences, RAH-1 antibody, and protocols for western blot and immunofluorescence. This work

was supported by Universidad Nacional del Noroeste de la Pcia de Bs. As. (UNNOBA); UNNOBA-CONICET under Grant PIO 2015-15720150100010CO; Instituto Nacional del Cancer, Ministerio de Salud under Grant ID31/2015; EU Horizon 2020 project RISE-2014 under Grant 645756; Subsidios de investigación bianuales, UNNOBA under Grant 01117/2017; and Fundación Alberto J. Roemmers 2018.

## Conflict of interest

The authors declare no conflict of interest.

## Author contributions

FMS, DLV, AI, IS, IC, and AB performed experiments. PG and VS contributed with essential human samples. FMS and LA planned experiments, analyzed data, and wrote the manuscript. MG and AP revised the paper. IS contributed with essential paper revision. LA conceived and designed the research. All authors gave their final approval for publication.

## References

- Spinelli FM, Vitale DL, Demarchi G, Cristina C & Alaniz L (2015) The immunological effect of hyaluronan in tumor angiogenesis. *Clin Transl Immunol* **4**, e52.
- Cyphert JM, Tremplus CS & Garantzotis S (2015) Size matters: molecular weight specificity of hyaluronan effects in cell biology. *Int J Cell Biol* **2015**, 563818.
- Rugg MS, Willis AC, Mukhopadhyay D, Hascall VC, Fries E, Fulop C, Milner CM & Day AJ (2005) Characterization of complexes formed between TSG-6 and inter-alpha-inhibitor that act as intermediates in the covalent transfer of heavy chains onto hyaluronan. *J Biol Chem* **280**, 25674–25686.
- Briggs DC, Birchenough HL, Ali T, Rugg MS, Waltho JP, Ievoli E, Jowitt TA, Enghild JJ, Richter RP, Salustri A *et al.* (2015) Metal ion-dependent heavy chain transfer activity of TSG-6 mediates assembly of the cumulus-oocyte matrix. *J Biol Chem* **290**, 28708–28723.
- Day AJ & Milner CM (2018) TSG-6: a multifunctional protein with anti-inflammatory and tissue-protective properties. *Matrix Biol* **78–79**, 68–83.
- Tammi RH, Kultti A, Kosma VM, Pirinen R, Auvinen P & Tammi MI (2008) Hyaluronan in human tumors: pathobiological and prognostic messages from cell-associated and stromal hyaluronan. *Semin Cancer Biol* **18**, 288–295.
- Cowman MK, Lee HG, Schwertfeger KL, McCarthy JB & Turley EA (2015) The content and size of hyaluronan in biological fluids and tissues. *Front Immunol* **6**, 261.

- 8 Delpech B, Chevallier B, Reinhardt N, Julien JP, Duval C, Maingonnat C, Bastit P & Asselain B (1990) Serum hyaluronan (hyaluronic acid) in breast cancer patients. *Int J Cancer* **46**, 388–390.
- 9 Yahya RS, El-Bindary AA, El-Mezayen HA, Abdelmasseh HM & Eissa MA (2014) Biochemical evaluation of hyaluronic acid in breast cancer. *Clin Lab* **60**, 1115–1121.
- 10 Singleton PA (2014) Hyaluronan regulation of endothelial barrier function in cancer. *Adv Cancer Res* **123**, 191–209.
- 11 Alaniz L, Garcia M, Rizzo M, Piccioni F & Mazzolini G (2009) Altered hyaluronan biosynthesis and cancer progression: an immunological perspective. *Mini Rev Med Chem* **9**, 1538–1546.
- 12 Bourguignon LY, Wong G, Earle CA & Xia W (2011) Interaction of low molecular weight hyaluronan with CD44 and toll-like receptors promotes the actin filament-associated protein 110-actin binding and MyD88-NFkappaB signaling leading to proinflammatory cytokine/chemokine production and breast tumor invasion. *Cytoskeleton* **68**, 671–693.
- 13 Ginhoux F & Jung S (2014) Monocytes and macrophages: developmental pathways and tissue homeostasis. *Nat Rev Immunol* **14**, 392–404.
- 14 Murdoch C & Lewis CE (2005) Macrophage migration and gene expression in response to tumor hypoxia. *Int J Cancer* **117**, 701–708.
- 15 Mantovani A, Marchesi F, Malesci A, Laghi L & Allavena P (2017) Tumour-associated macrophages as treatment targets in oncology. *Nat Rev Clin Oncol* **14**, 399–416.
- 16 Sokolowska M, Chen LY, Eberlein M, Martinez-Anton A, Liu Y, Alsaaty S, Qi HY, Logun C, Horton M & Shelhamer JH (2014) Low molecular weight hyaluronan activates cytosolic phospholipase A2alpha and eicosanoid production in monocytes and macrophages. *J Biol Chem* **289**, 4470–4488.
- 17 Rayahin JE, Buhrman JS, Zhang Y, Koh TJ & Gemeinhart RA (2015) High and low molecular weight hyaluronic acid differentially influence macrophage activation. *ACS Biomater Sci Eng* **1**, 481–493.
- 18 Milner CM & Day AJ (2003) TSG-6: a multifunctional protein associated with inflammation. *J Cell Sci* **116**, 1863–1873.
- 19 Mittal M, Tiruppathi C, Nepal S, Zhao YY, Grzych D, Soni D, Prockop DJ & Malik AB (2016) TNFalpha-stimulated gene-6 (TSG6) activates macrophage phenotype transition to prevent inflammatory lung injury. *Proc Natl Acad Sci USA* **113**, E8151–E8158.
- 20 Bredholt G, Mannelqvist M, Stefansson IM, Birkeland E, Bo TH, Oyan AM, Trovik J, Kalland KH, Jonassen I, Salvesen HB *et al.* (2015) Tumor necrosis is an important hallmark of aggressive endometrial cancer and associates with hypoxia, angiogenesis and inflammation responses. *Oncotarget* **6**, 39676–39691.
- 21 Swinson DE, Jones JL, Richardson D, Cox G, Edwards JG & O'Byrne KJ (2002) Tumour necrosis is an independent prognostic marker in non-small cell lung cancer: correlation with biological variables. *Lung Cancer* **37**, 235–240.
- 22 Leek RD, Landers RJ, Harris AL & Lewis CE (1999) Necrosis correlates with high vascular density and focal macrophage infiltration in invasive carcinoma of the breast. *Br J Cancer* **79**, 991–995.
- 23 Deryugina EI & Quigley JP (2015) Tumor angiogenesis: MMP-mediated induction of intravasation- and metastasis-sustaining neovasculature. *Matrix Biol* **44–46**, 94–112.
- 24 Day AJ & de la Motte CA (2005) Hyaluronan cross-linking: a protective mechanism in inflammation? *Trends Immunol* **26**, 637–643.
- 25 Zhang S, He H, Day AJ & Tseng SC (2012) Constitutive expression of inter-alpha-inhibitor (IalphaI) family proteins and tumor necrosis factor-stimulated gene-6 (TSG-6) by human amniotic membrane epithelial and stromal cells supporting formation of the heavy chain-hyaluronan (HC-HA) complex. *J Biol Chem* **287**, 12433–12444.
- 26 Shrimali RK, Yu Z, Theoret MR, Chinnasamy D, Restifo NP & Rosenberg SA (2010) Antiangiogenic agents can increase lymphocyte infiltration into tumor and enhance the effectiveness of adoptive immunotherapy of cancer. *Can Res* **70**, 6171–6180.
- 27 Jiang D, Liang J & Noble PW (2011) Hyaluronan as an immune regulator in human diseases. *Physiol Rev* **91**, 221–264.
- 28 Mytar B, Woloszyn M, Szatanek R, Baj-Krzyworzeka M, Siedlar M, Ruggiero I, Wieckiewicz J & Zembala M (2003) Tumor cell-induced deactivation of human monocytes. *J Leukoc Biol* **74**, 1094–1101.
- 29 del Fresno C, Otero K, Gomez-Garcia L, Gonzalez-Leon MC, Soler-Ranger L, Fuentes-Prior P, Escoll P, Baos R, Caveda L, Garcia F *et al.* (2005) Tumor cells deactivate human monocytes by up-regulating IL-1 receptor associated kinase-M expression via CD44 and TLR4. *J Immunol* **174**, 3032–3040.
- 30 Zhang G, Guo L, Yang C, Liu Y, He Y, Du Y, Wang W & Gao F (2016) A novel role of breast cancer-derived hyaluronan on induction of M2-like tumor-associated macrophages formation. *Oncimmunology* **5**, e1172154.
- 31 Bertani FR, Mozetic P, Fioramonti M, Iuliani M, Ribelli G, Pantano F, Santini D, Tonini G, Trombetta M, Businaro L *et al.* (2017) Classification of M1/M2-polarized human macrophages by label-free hyperspectral reflectance confocal microscopy and multivariate analysis. *Sci Rep* **7**, 8965.
- 32 Dirx AE, Oude Egbrink MG, Wagstaff J & Griffioen AW (2006) Monocyte/macrophage infiltration in tumors: modulators of angiogenesis. *J Leukoc Biol* **80**, 1183–1196.

- 33 Xu J, Rodriguez D, Petitclerc E, Kim JJ, Hangai M, Moon YS, Davis GE & Brooks PC (2001) Proteolytic exposure of a cryptic site within collagen type IV is required for angiogenesis and tumor growth in vivo. *J Cell Biol* **154**, 1069–1079.
- 34 Takahashi K, Eto H & Tanabe KK (1999) Involvement of CD44 in matrix metalloproteinase-2 regulation in human melanoma cells. *Int J Cancer* **80**, 387–395.
- 35 Zhong X, Chen B & Yang Z (2018) The role of tumor-associated macrophages in colorectal carcinoma progression. *Cell Physiol Biochem* **45**, 356–365.
- 36 Choi J, Gyamfi J, Jang H & Koo JS (2018) The role of tumor-associated macrophage in breast cancer biology. *Histol Histopathol* **33**, 133–145.
- 37 Wahl LM & Smith PD (2001) Isolation of Monocyte/Macrophage Populations in Current Protocols in Immunology. John Wiley & Sons Inc, Hoboken, NJ.
- 38 Fujimoto T, Savani RC, Watari M, Day AJ & Strauss JF III (2002) Induction of the hyaluronic acid-binding protein, tumor necrosis factor-stimulated gene-6, in cervical smooth muscle cells by tumor necrosis factor-alpha and prostaglandin E(2). *Am J Pathol* **160**, 1495–1502.
- 39 Alaniz L, Garcia M, Cabrera P, Arnaiz M, Cavaliere V, Blanco G, Alvarez E & Hajos S (2004) Modulation of matrix metalloproteinase-9 activity by hyaluronan is dependent on NF-kappaB activity in lymphoma cell lines with dissimilar invasive behavior. *Biochem Biophys Res Comm* **324**, 736–743.
- 40 Pasarica M, Sereda OR, Redman LM, Albarado DC, Hymel DT, Roan LE, Rood JC, Burk DH & Smith SR (2009) Reduced adipose tissue oxygenation in human obesity: evidence for rarefaction, macrophage chemotaxis, and inflammation without an angiogenic response. *Diabetes* **58**, 718–725.